

Dynamic Shock Wave Reflection

Luke T. Felthun* and Beric W. Skews†

University of the Witwatersrand, Johannesburg 2050, South Africa

The study of the transition from regular to Mach reflection of shock waves has received considerable attention over the past decade, particularly because of the differences found between numerical and experimental data sets. Whereas this has now been satisfactorily shown to be due to wind-tunnel noise, it raises the issue of the effects of unsteady, or dynamic, effects on transition. These are also of interest because they can arise both due to the reflecting surface changing incidence resulting from steady body motion over a surface of variable slope, or due to changes in angle of incidence of the body itself. In this study, a moving-body numerical scheme was used to study the transition between regular and Mach shock wave reflections on a plane surface in steady supersonic flows under different rates of body incidence change. A wedge in a steady supersonic flow was used to generate an oblique shock wave that was reflected off of an ideal boundary. When the angle of the wedge was varied slowly, transition occurred close to the theoretical limit for each reflection type, that is, at the von Neumann criterion for transition from Mach reflection and at detachment for transition from regular reflection. At higher rates of wedge rotation, transition to Mach reflection occurred at angles beyond the detachment criterion, indicating that the steady-state assumption used to predict detachment breaks down as the rate of change of the incident wave angle is increased. When transitioning from Mach reflection, rapidly reducing the wedge angle results in the development of an inverse Mach reflection that eventually terminates below the von Neumann condition. In these cases, transitional waves are observed that develop to accommodate the discontinuous changes in state required when transition occurs away from the von Neumann condition.

Introduction

IN steady flows, two types of shock wave reflections can occur, a regular reflection and a Mach reflection¹ (Fig. 1). To assist in describing these geometries, the (p, θ) shock polar is used. This plots the relationship between the pressure across an oblique shock wave and the deflection angle of the flow across the wave. Although such polars strictly apply to steady and pseudosteady flows, they can be useful in explaining the behavior encountered in unsteady flows, as shall be done later, but then only in a qualitative sense. Figure 2 shows a number of polars calculated for an incident flow Mach number of 3.0, corresponding to the general cases of regular and Mach reflection shown in Fig. 1. State 0 is the oncoming supersonic flow; state 1, that between the incident and reflected shocks; state 2, that behind the reflected shock; and state 3, that behind the Mach stem at the triple point, for Mach reflection. The polars for a typical regular reflection are given in Fig. 2a.

There are several criteria that attempt to predict when one reflection type will transition to the other. The detachment criterion, shown in Fig. 2c, gives the highest deflection angle for which a regular reflection is possible. Beyond this angle, the reflected wave is no longer able to turn the flow behind the reflected wave parallel to the wall, forcing the reflection point to detach from the wall. A further criterion, the sonic criterion, suggests that transition occurs when the flow behind the reflected shock goes sonic. This occurs a fraction of a degree before detachment, and it is usually impossible to distinguish experimentally between the two criteria. In this case, the reflected wave polar in Fig. 2c would be fractionally shifted to the left.

Should transition occur at the sonic or detachment point, a discontinuous change of state has to take place between the regular

reflection state (at A), where the reflected polar crosses the vertical axis, to the Mach reflection state (at B), located where the reflected polar crosses the incident polar. This consideration is an important issue in this study, because, unlike most previous work that examines steady flows on either side of the transition, here the transition is passed through in a continuous manner. Because a discontinuous change of state of the reflected wave had yet to be observed, Henderson and Lozzi² required that the criterion should allow for a continuous transition between regular and Mach reflection. This can only occur where the regular and Mach reflection solutions coincide, that is, where the reflected polar intersects the incident polar and the vertical axis at the same point (Fig. 2d). This is referred to as the mechanical equilibrium or the von Neumann criterion. This state also represents the limit at which a Mach reflection can exist, being the point at which the flow behind the Mach stem becomes parallel to the wall. If the wedge angle had to decrease, moving the reflected polar to the left, the flow behind the Mach stem would be directed away from the wall. This results in an inverse Mach reflection, which is not possible in a steady flow because in such a case the triple point will be moving toward the wall and will terminate on reaching the wall.

It is evident that between the limiting cases identified in Figs. 2c and 2d, both regular and Mach reflection are possible, and this region is referred to as the dual solution domain. Hornung et al.³ proposed that if the incident wave angle was changed smoothly, transition would occur at the von Neumann criterion when transitioning from a Mach reflection and at detachment when transitioning from a regular reflection. As different paths are followed, depending on the direction being taken, this is referred to as the hysteresis phenomenon. Such hysteresis was first demonstrated numerically by Chpoun et al.⁴ and subsequently by many others. The common practice in these tests has been that once an initial steady-state solution had been obtained for the initial wedge angle, the wedge is impulsively moved through a small angle and the flow was then allowed to converge to steady state again. Thus, the dynamics of the transition were not examined. Using a moving boundary code, Khotyanovsky et al.⁵ were able to perform these tests using a continuous motion for a Mach 5 flow and thereby indicate some of the true dynamic effects, as will be discussed later.

Experimental studies of the hysteresis phenomenon have met with varying success, with the differences currently being primarily ascribed to wind-tunnel noise because a number of workers have

Presented as Paper 2002-0549 at the AIAA 40th Aerospace Sciences Meeting, Reno, NV, 14–17 January 2002; received 23 July 2003; revision received 16 March 2004; accepted for publication 6 April 2004. Copyright © 2004 by the American Institute of Aeronautics and Astronautics, Inc. All rights reserved. Copies of this paper may be made for personal or internal use, on condition that the copier pay the \$10.00 per-copy fee to the Copyright Clearance Center, Inc., 222 Rosewood Drive, Danvers, MA 01923; include the code 0001-1452/04 \$10.00 in correspondence with the CCC.

*Research Student, School of Mechanical, Industrial, and Aeronautical Engineering; currently Development Engineer, Fluent, Inc., 10 Cavendish Court, Centerra Resource Park, Lebanon, NH 03766-1442.

†Director, Flow Research Unit, School of Mechanical, Industrial, and Aeronautical Engineering. Member AIAA.

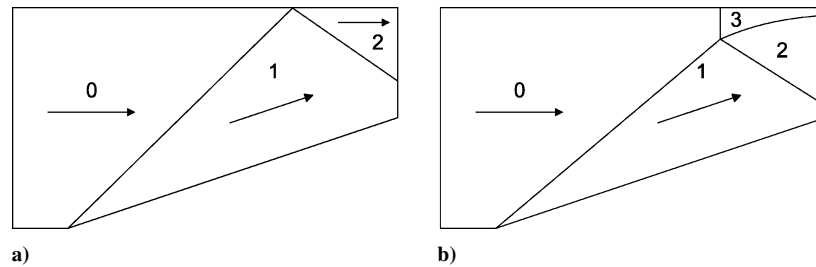


Fig. 1 Possible reflection configurations in steady flows: a) regular reflection and b) Mach reflection.

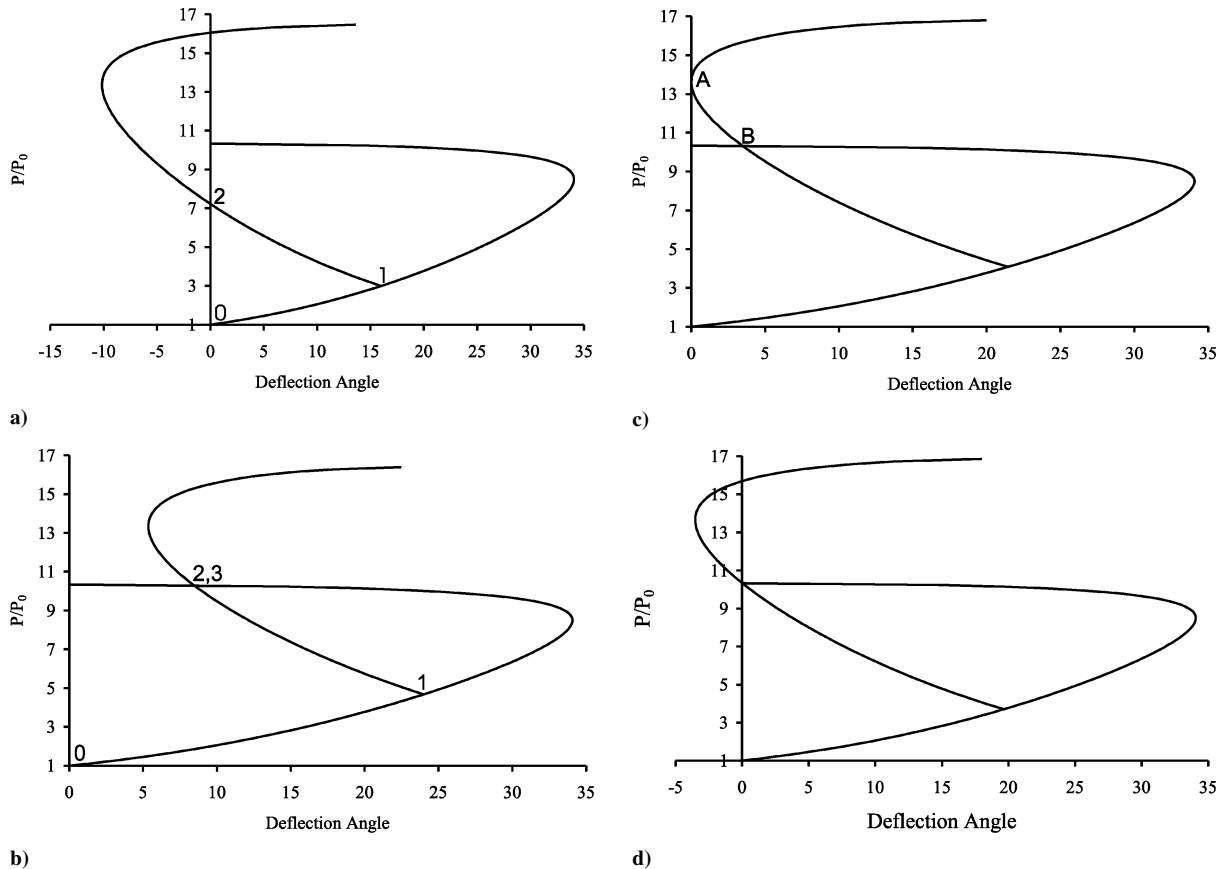


Fig. 2 Typical reflection configurations in steady flow, $M = 3.0$: a) regular reflection, b) Mach reflection, c) detachment criterion, and d) von Neumann criterion.

shown that flow perturbations do affect transition. A comprehensive review of the field has recently been given by Ben-Dor et al.⁶

Numerical Scheme and Hysteresis Tests

A vertex-centered arbitrary Lagrangian Eulerian finite volume scheme on unstructured triangular meshes was developed to perform the simulations in this work. Fluxes across cell interfaces were calculated with the AUSM+ flux function, written in terms of a moving reference frame. The gradient reconstruction scheme of Luo et al.⁷ in conjunction with the multidimensional limiter of Barth and Jespersen⁸ was used to reconstruct higher-order-accurate solutions at the cell interfaces. To calculate the flux balance in the deforming cells correctly, the geometric conservation law was satisfied by the use of the time-averaged normals method of Nkonga and Guillard.⁹ A four-step explicit Runge–Kutta scheme was used to advance the solution in time. The mesh was moved at each time step with Laplacian smoothing. At regular time intervals, the mesh was adapted by the use of direct point insertion, edge collapsing, and edge swapping.

Similar numerical tests to those of Khotyanovsky et al.⁵ for a Mach 5 flow have been undertaken with the present code for a

continuously rotating wedge in a steady supersonic Mach 3 flow. This is both to check the code for its ability to produce hysteresis and to check transition conditions against steady flow theory, for very slow wedge motion. Subsequent sections will deal with the dynamic effects resulting from much more rapid wedge motion. At this Mach number, detachment occurs at a wave angle of 39.5 deg, corresponding to a wedge angle of 21.5 deg, and the von Neumann criterion occurs at a wave angle of 37.4 deg, corresponding to a wedge angle of 19.7 deg.

Two numerical tests are performed to demonstrate hysteresis. In the first test, the simulation is started with a steady-state regular reflection, and then the wedge angle is increased until transition to Mach reflection is achieved. The second test is started with a steady Mach reflection, and the wedge angle is decreased until the Mach reflection transitions to a regular reflection. In both of these tests, the wedge is rotated slowly about its leading edge, so that throughout the simulation the essentially unsteady solution corresponds to the steady-state solution at every wedge angle. To describe the rotation of the wedge in a nondimensional manner, the tests are parameterized in terms of a trailing-edge Mach number M_t , that is, the absolute velocity of the trailing edge with respect to the fixed leading edge for

a chord of unity, divided by the freestream speed of sound. In both of these tests the wedge is moved such that the trailing-edge Mach number is 0.001. The back of the wedge has been extended from the trailing edge to the full length of the computational domain, so that no downstream subsonic areas are developed that would complicate the outlet boundary conditions. No transient effects were observable in these tests, this being determined by measurement of the incident wave angle at the wedge and at the point of reflection, and by confirmation that they did not deviate from the angle predicted by steady-state calculations. If the wedges were moved much faster, these angles would begin to lag behind the steady-state value, with the angle at the point of reflection deviating further than the angle at the wedge apex as the incident wave began to curve.

In these tests, the initial steady-state result was obtained with the standard practice of impulsive imposition of a uniform flowfield at freestream conditions on the domain and by allowing the solution to converge to steady state. It is found that whenever the wedge angle was in the dual solution domain, the regular reflection solution was obtained. When converging to steady state by the use of impulsive starting conditions, the leading-edge shock wave will be initiated on the wedge with the same angle as the wedge. It will then proceed to steepen until it reaches the steady-state angle. This means that when the wave first starts to reflect off of the upper wall, the shock wave angle will be much smaller than the steady-state result, typically below the von Neumann criterion, resulting in a regular reflection. Once a regular reflection is established, it remains a regular reflection throughout the dual solution domain. For this reason, when impulsive starting conditions are used, as long as a regular reflection is possible (that is, below detachment), a regular reflection will always be obtained. This made it possible in the tests modeling transition from regular to Mach reflection to start within the dual solution domain, in this case, 20 deg. A few additional simulations were conducted with an initial angle of 12 deg to establish the influence of this lower starting angle. When a Mach reflection was required for the initial condition, an initial angle of 23 deg was used. As a consequence, when a Mach reflection was desired as an initial condition, a steady-state solution outside the dual solution domain had to be obtained.

Convergence to steady state by the use of impulsive starting conditions differs from what is more likely to occur in many physical situations. In practice, a flow is more likely to start with a slow velocity and be accelerated until the steady-state velocity is achieved. Under these conditions, an incident shock wave will initially be formed with a fairly large wave angle and will form a Mach reflection. This Mach reflection will then persist throughout the dual solution domain. It seems, therefore, that when flow conditions are such that dual solutions are possible, it is necessary to carefully consider how steady-state solutions are reached.

In the regular to Mach reflection test (Figs. 3a–3c) transition was observed at 21.7 deg, 0.2 deg above the theoretical value and in the Mach to regular reflection case (Figs. 3d–3f) transition was observed at 20 deg, 0.3 deg below the theoretical value. In these cases, it can be said that these values do nominally correspond to the theoretical limits in the steady case, and that shock waves maintain their configuration in the dual solution domain. Transition occurring at different angles for each of these tests confirms the existence of

the dual solution domain. This is demonstrated in Figs. 3b and 3e, where, in both cases, the wedge angle is at 21 deg, but a regular reflection exists in the first case and a Mach reflection in the second.

However, there is still a small discrepancy showing a bias toward regular reflection in both tests, that is, with the regular reflection persisting beyond detachment but transitioning early from Mach reflection. This may be partially related to the difficulty in determination from the contour plots when a Mach reflection has actually started, resulting in a slight observational bias toward regular reflection. In general, however, tests run at lower resolutions result in larger errors biased toward regular reflections. Thus, the inability of the solver to resolve a Mach reflection will increase as coarser meshes are used. This issue is addressed later. Although there is still the possibility of transient effects, we believe that they are minor.

Thus, both the hysteresis phenomenon and the correct transition angles are obtained for these slow wedge rotation simulations.

Dynamic Transition from Regular to Mach Reflection

In this section, the regular to Mach reflection case is modeled with more rapidly rotating wedges, so that time-dependent effects on the development of a Mach reflection could be observed. Increasing the velocity of the wedge will affect the flow in a couple of ways. First, the incident shock wave angle will begin to lag behind the steady-state value for the current wedge angle. The incident shock wave will curve along its length, with the deviation from the steady-state value increasing with distance from the wedge apex. This means that there is no longer a direct relationship between the flow deflection angle at the wedge and the incident wave angle at the point of reflection, and it becomes necessary to relate all transition criteria to the wave angle at the point of reflection. Figure 4 shows this effect for anticlockwise wedge rotation. Rapid clockwise rotation will result in corresponding concave curvature to the oncoming flow. Khotyanovsky et al.⁵ have performed some computations for a continuously rotated wedge in a flow at Mach 5, with the wedge being rotated around the trailing edge, and noted this shock curvature at the higher rotational speeds. However, they did not examine the consequence of this rotation on the dynamics of the wave reflection. Some insight into the mechanisms whereby rapid wedge rotation influences the flow has been given by Markelov et al.¹⁰ They solved the Boltzman equation for a rarefied gas at a freestream Mach number of 4.96. Their interest was primarily on the effect of possible

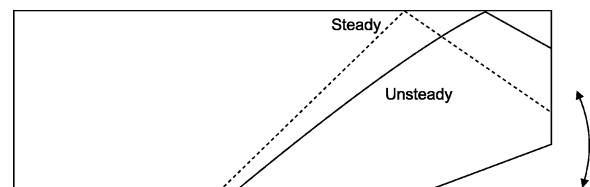


Fig. 4 Incident shock wave on a rotating wedge.

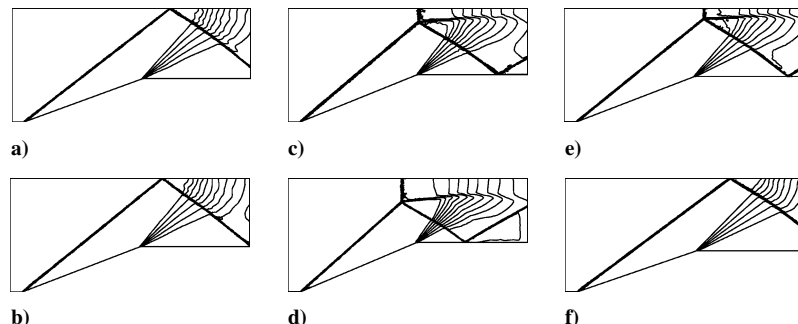


Fig. 3 Transition from regular to Mach reflection ($M_t = 0.001$): a) $\theta = 20$, b) 21, c) 22, d) 23, e) 21, and f) 19 deg.

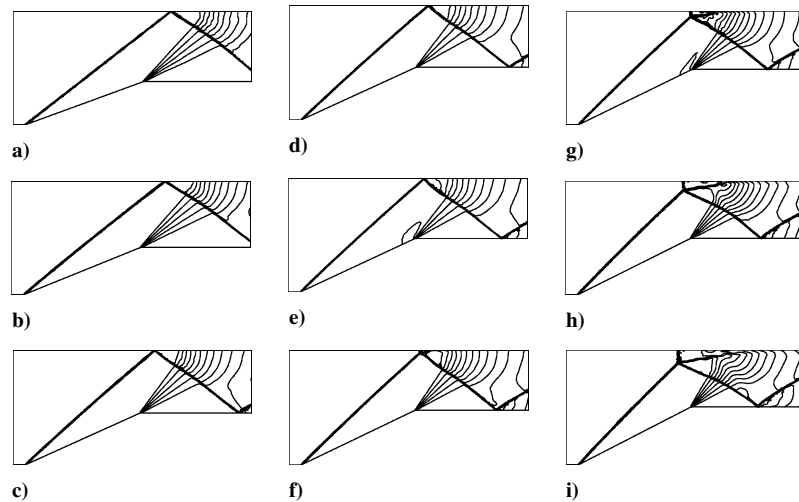


Fig. 5 Transition from regular to Mach reflection ($M_t = 0.05$): a) $\theta = 20$, b) 22, c) 24, d) 24.5, e) 25, f) 25.5, g) 26, h) 26.5, and i) 27 deg.

wind-tunnel model vibration on transition. After an initial steady flow was achieved they impulsively rotated the wedge at a constant angular speed over a 1-deg arc and then stopped it impulsively. This generated compression and expansion waves that interacted with the incident shock, resulting in the wave curvature. They also did not examine the effects of continuous rotation on the transition process.

With reference to Fig. 4, as the wedge angle increases, the reflection point will move to the left, toward the oncoming flow. Because the transition calculations are based on a reference frame fixed to the reflection point, the Mach number of the incident flow is effectively increased. Unfortunately, it is not straightforward to make an a priori prediction of the velocity of the reflection point. If it were assumed that the incident shock did not lag behind the steady-state value significantly, the velocity of the reflection point could be calculated as a function of wedge trailing-edge velocity by simple use of the wave angle/deflection angle relationships for steady supersonic flow and basic trigonometric relationships. This prediction would be increasingly inaccurate at higher wedge velocities because the incident wave angle increasingly lags behind the steady-state solution. One possibility is to determine the velocity of the reflection at transition from the numerical solution and then to recalculate the transition criteria. However, at Mach numbers of about 2.5 and higher, both the sonic and detachment criterion angles are nearly constant as a function of Mach number. For example, increasing the Mach number from 3.0 to 3.2 decreases the detachment criterion angle from 39.52 to 39.38 deg. Given the resolution of the simulations and measuring inaccuracies, it was decided to ignore the effect that this would have on the transition angles. However, at lower Mach numbers, the detachment angle varies more significantly with changes in Mach number, and, in such circumstances, the velocity of the reflection point would need to be taken into consideration.

A series of 10 tests were performed with trailing-edge Mach numbers varying from 0.01 to 0.1. Density contour plots from the $M_t = 0.05$ test are shown in Fig. 5. The steady-state solution at 20 deg is shown in Fig. 5a. The influence of the unsteady motion becomes evident in the changing of the position of the reflected shock at the outlet boundary in Figs. 5b and 5c. In Figs. 5c–5e, a steepening of the reflected shock wave immediately behind the reflection point can be seen. If one uses steady-state considerations, this indicates that the reflected wave has moved into the strong shock regime. Pressure measurements taken in this vicinity show a significant increase of pressure that reinforces the possibility. This has also been noted by Markelov et al.¹⁰ The reflected wave becomes markedly curved and the flow behind it nonuniform.

Immediately after transition occurs, a kink can be seen in the reflected shock wave, which propagates down the shock wave away from the reflection. This can be seen in Figs. 5f and 5g but tends to be too weak to be observable in the later contour plots. As discussed earlier, when transition occurs away from the von Neumann crite-

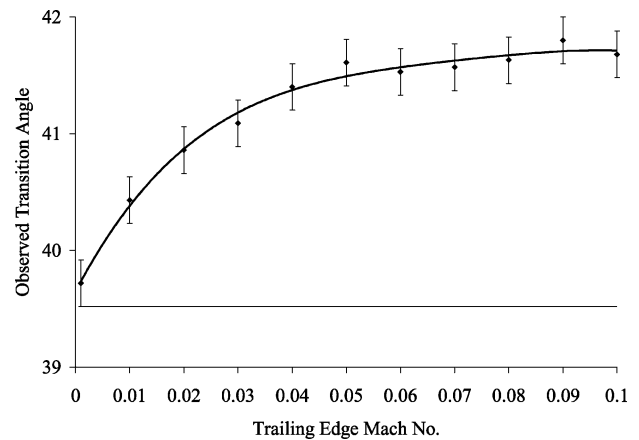


Fig. 6 Effect of trailing-edge Mach number on transition from regular to Mach reflection.

rion, a discontinuous change in state has to take place. In this case, a drop in pressure has to take place. This pressure drop is accommodated by a shock wave that propagates down the reflected shock, at a speed slower than the local flow velocity. The shock wave, which is relatively weak, appears to degenerate into a compression wave resulting in a more gentle curvature in the reflected shock wave later in the simulation (Figs. 5h and 5i).

If the wedge is stopped during these tests, in general, the flow would converge to the expected steady-state solution. However, at wedge angles above 25 deg a steady supersonic solution is not possible due to the choking of the flow. One consequence of the moving wedge tests is that choking is delayed. Whenever the motion of the wedge was stopped at these angles and the solution allowed to converge to steady state, the Mach stem grew until it formed a normal shock across the full height of the section that traveled upstream, changing the flow conditions to subsonic.

The wedge angle θ and incident wave angle β , when transition was observed, are shown in Table 1 and Fig. 6. It must be reiterated that incident wave angles are measured at the reflection point, not at the wedge leading edge. Results from the simulations were recorded at intervals of 0.1 deg. These tests were started with a wedge angle of 20 deg. The estimated accuracy of measurements is ± 0.2 deg. Measurements were taken within the graphics package by zooming in on high-resolution contour plots, checking for repeatability, and comparing measured results for those steady cases where theoretical values are known. In these simulations, transition is observed at angles higher than those predicted by the detachment criterion. The difference between the detachment angle and when transition is observed increases with increasing trailing-edge Mach number,

Table 1 Transition conditions

M_t	0.01	0.02	0.03	0.04	0.05	0.06	0.07	0.08	0.09	0.10
θ	22.6	23.4	24	24.7	25.2	25.6	26.1	26.6	27	27.6
β	40.43	40.86	41.09	41.4	41.61	41.53	41.57	41.63	41.8	41.68

Table 2 Evolution of Mach stem

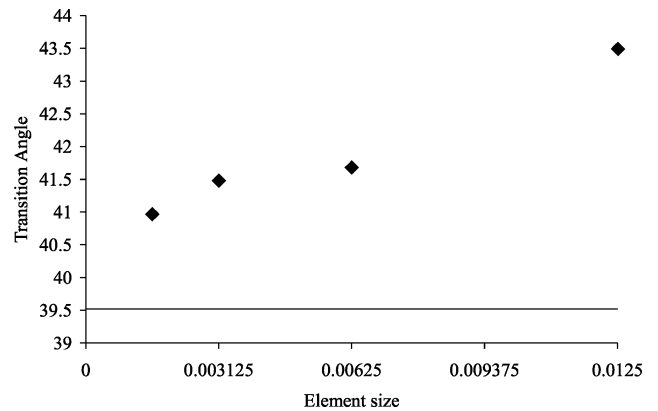
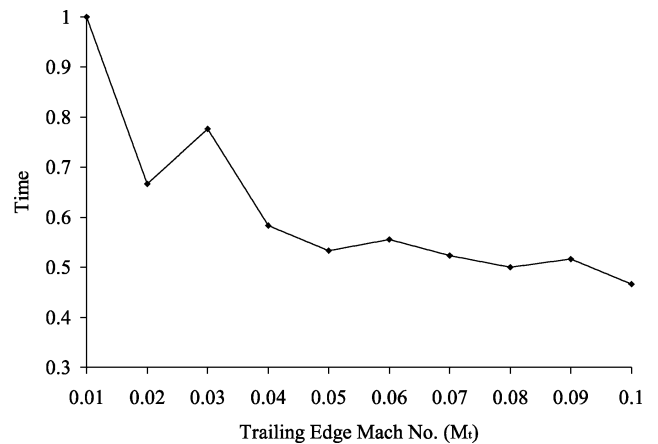
M_t	0.01	0.02	0.03	0.04	0.05	0.06	0.07	0.08	0.09	0.10
θ_h , deg	21.8	23.8	24.7	25.4	26	26.6	27.2	27.8	28.4	29.0
β_h , deg	41.11	41.31	42.09	42.5	42.81	43.31	43.46	43.54	43.52	43.72
$\delta\theta_h$	0.3	0.4	0.7	0.7	0.8	1.0	1.1	1.2	1.4	1.4
$\delta\beta_h$	0.68	0.48	1.0	1.1	1.2	1.78	1.89	1.91	1.72	2.04

leveling off, however, at the higher trailing-edge Mach numbers at just over 2 deg past detachment. This is shown in Fig. 6 with a fourth-order curve fit superimposed. It was expected that a different initial angle could affect the transition value, and so simulations were run for trailing-edge Mach numbers of 0.02, 0.05, and 0.1 and a 12-deg starting angle. The results are nearly identical to those at 20 deg. This would suggest that the shock curvature due to the initial starting impulse, compared to that due to the steady rotation, did not get near to the transition angles. This could well be different for a wedge leading edge at a different distance from the reflection plane. This influence has not yet been investigated.

The first possible cause of the delay in transition that must be considered is that of numerical resolution. As mentioned earlier, if the numerical resolution is inadequate to resolve the Mach stem, a regular reflection will be observed. It was observed in these tests that the Mach stems gets progressively smaller, relative to the incident wave angle, as the wedge rotation rate is increased. It is reasonable, therefore, to expect that the error in prediction of transition would increase as the wedge rotation rate is increased. It must be determined whether this is the primary cause of the delay in transition being observed or just a secondary effect. To assess the effect of resolution on the angle at which transition is observed, the $M_t = 0.1$ test was repeated at two different resolutions, one at one-half the resolution and the other at twice the resolution of the preceding tests. It was only practical to run this test at the higher resolution because the timescale modeled was not as long as in the other, slower moving wedge tests. Halving the resolution resulted in the angle at which transition was observed increasing by 1.81 deg to 43.49 deg. However, doubling the resolution resulted in the transition angle decreasing by only 0.2 deg to 41.48 deg. It would be reasonable to expect that if inadequate resolution were the primary factor in the transition angle deviating from the theoretical predicted result, doubling the resolution would have a far greater impact on the result. As can be seen in Fig. 7, as the mesh is refined by a decrease in the minimum element size (expressed in relation to the length of the wedge), the transition angle does not appear to converge to the steady flow detachment criterion, shown by the horizontal line.

If the delay in transition being observed was simply the failure to resolve a Mach stem, it is feasible that there would be a relationship between the delay in observed transition and the rate of growth of the Mach stem, with the Mach stem only becoming resolvable once it reached a certain size. For this reason, a series of measurements were taken so that an understanding of the evolution of a Mach stem with changing incident angle could be obtained. The delay in transition angle increased steadily with increasing wedge rotation rate from detachment until it leveled off at roughly 2 deg above detachment. If, as the wedge rotation rate was increased, the rate at which the Mach stem grew increased proportionally, and delayed Mach stem growth were the cause of the delay, this would result in the leveling off observed in the result.

To determine how the growth of the Mach stem is affected by the changing incident wave angle, a series of measurements were taken in which the change in incident wave angle from the point where transition is first observed and where the Mach stem reaches a height equal to 0.15 times the characteristic length is measured.

**Fig. 7 Relationship between transition angle and element size for $M_t = 0.1$.****Fig. 8 Mach stem height.**

This height is the maximum height achieved in the $M_t = 0.1$ test at 29 deg, which is equal to 0.14 times the length of the wedge. The results are shown in Table 2: θ_h = wedge angle when Mach stem reaches prescribed height; β_h = incident wave angle when Mach stem reaches prescribed height; $\delta\theta$ = wedge angle at transition - θ_h ; and $\delta\beta$ = incident wave angle at transition - β_h . The time taken from observed transition to the specified height is also calculated and normalized against the time for the $M_t = 0.01$ test. The time taken for the Mach stem to grow to the specified height vs the trailing-edge Mach number is plotted in Fig. 8. This shows that the time taken for the Mach stem to reach the specified height initially decreases, but eventually becomes constant, becoming independent of the wedge rotation rate and, consequently, of the incident wave angle. If the rate of Mach stem growth were the cause of numerical errors, this characteristic would likely cause the observed transition angle to increase linearly with increasing wedge rotation rate, which is not the case.

Note that in our attempt to compare Mach stem growth rate with a delay in transition being observed, there is an implicit assumption that an unresolved Mach stem displays similar growth behavior as a resolved Mach stem. Because this is largely unknown, the preceding result does not necessarily preclude Mach stem growth rate as a primary influence. The results simply do not support that conjecture. The Mach stem growth rate is an interesting characteristic in its own right and is worth further study. To eliminate conclusively the possibility that insufficient resolution is the cause of the delay in transition, it would be necessary to repeat these tests at significantly higher resolutions. However, the preceding results indicate that it is likely that this is not the primary source of the discrepancies.

The theoretical shock wave analysis used up to this point is only valid for plane waves in a steady flow in a frame fixed to the reflection point and, is, thus, not strictly applicable to the unsteady flows examined. A couple of factors contribute to the differences. The polar represents the locus of all states achievable from a given initial state,

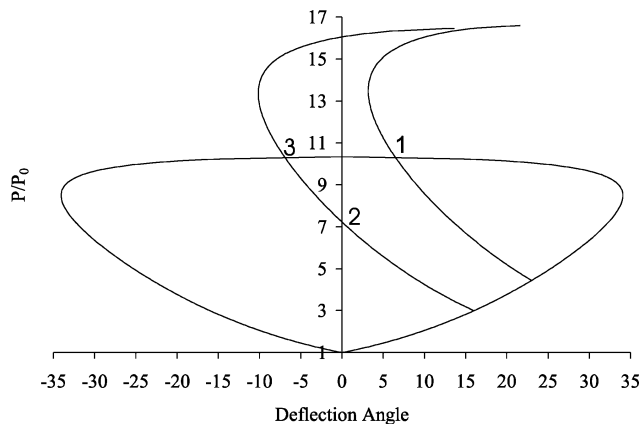


Fig. 9 Inverse Mach reflection polars.

and, in the dynamic case treated here, this initial state is changing in time. There is a delay in the propagation of information about the change of wedge position reaching the reflection point. Thus, there are weak compression waves emanating from the surface of the wedge that cause the steepening of the incident wave. Once the reflected wave has passed the sonic criterion, the downstream flow conditions will also have an influence. Whereas the application to highly unsteady shock wave problems of a simple moving reference frame has been widely used, this is mainly done for flows that are self-similar in time, or nearly so.

Furthermore, as noted earlier, the absolute Mach number of the flow relative to the reflection point also changes in time and, thus, so does the polar, due to reflection point movement. The equations on which shock polars are based take no account of the effects of flow acceleration and where the incident shock wave angle is changing in time. Nevertheless, it is helpful in the discussion and explanation of dynamic reflection phenomena to use the polar in a qualitative fashion.

Dynamic Transition from Mach to Regular Reflection

In this section, the effect of a rapid decrease in the wedge angle on the transition from Mach to regular reflection is examined. A detailed parametric study has not been performed for this case; only the general behavior of the flow will be examined as it transitions from Mach to regular reflection. For this case, we start with a steady-state Mach reflection at 23 deg and choose to finish with a regular reflection at 16 deg. The wedge will be moved rapidly, with a trailing-edge Mach number of 0.05, to ensure that transient effects will be displayed. The shock polars representing the starting and finishing steady states are shown in Fig. 9. The initial Mach reflection is represented by state one on this plot and the final regular reflection by state two. A primary issue of interest is the path that will be taken between these two states in this simulation.

Contour plots from this simulation are shown in Figs. 10 and 11. Mach contours are plotted in Figs. 10 and 11 because they show the path of the slipstream more clearly than density contours.

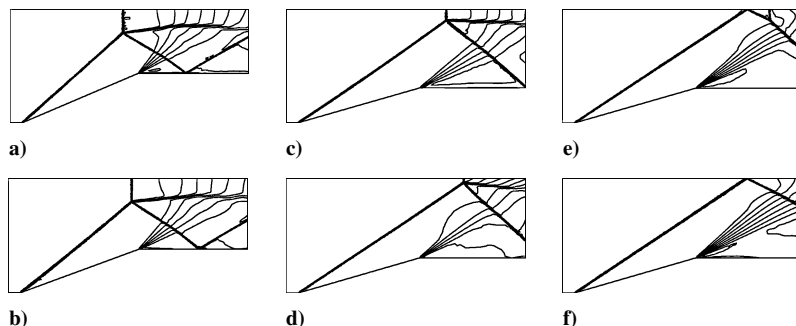


Fig. 10 Transition from Mach to regular reflection ($M_t = 0.05$): a) $\theta = 23$ and b) 20 deg; c) $\theta = 16$ deg and $T = 0$, d) $\theta = 16$ deg and $T = 0.4$, e) $\theta = 16$ deg and $T = 0.8$, and f) $\theta = 16$ deg and $T = 1.2$.

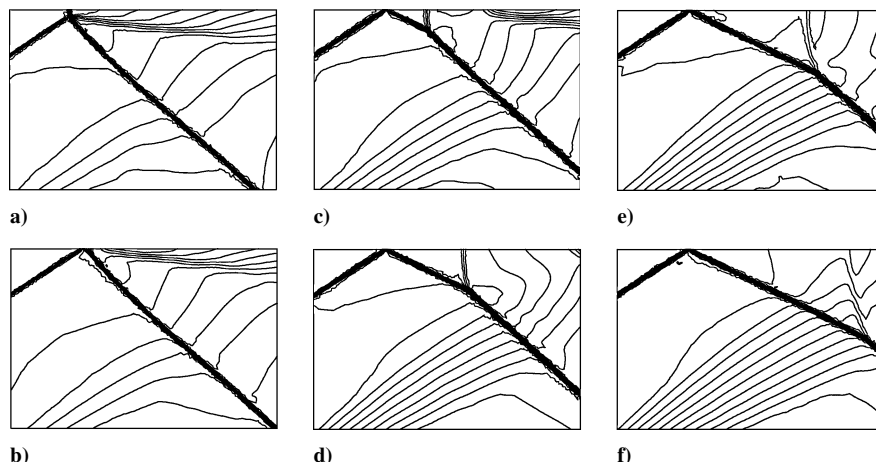


Fig. 11 Discontinuous Mach to regular reflection transition ($\theta = 16$ deg): a) $T = 0.5$, b) 0.6, c) 0.7, d) 0.8, e) 0.9, and f) 1.0.

In the first stage of the simulation, shown in Figs. 10a–10c, the wedge angle is reduced from 23 to 16 deg. At 16 deg, when the wedge rotation is stopped, an incident shock wave angle of 35.54 deg is measured at the triple point, and it is noted that the incident shock is concave to the oncoming flow. This value is still greater than the steady-state value of 33.29 deg but is smaller than the von Neuman criterion angle under these conditions of 37.36 deg. This means that the reflected shock polar intersects the incident shock polar to the left of the vertical axis. This indicates that the flow behind the Mach stem in the vicinity of the triple point, with respect to a reference frame connected to the triple point, is directed away from the reflecting surface. This state is called an inverse Mach reflection. Under these conditions, the triple point will always be moving toward the reflecting surface, with the Mach reflection terminating on reaching the wall. As a result, it is a purely transient phenomenon that cannot exist in steady flows. The direction of the slipstream, which is always in the direction of the flow relative to the triple point, can be clearly seen in Fig. 10c to be directed away from the wall. The direction of the slipstream can always be used as an indication of the nature of the Mach reflection.

As the wedge angle is reduced, the Mach stem actually grows slightly, reaching a maximum height at approximately 20 deg (Fig. 10b) before it starts reducing in height. The motion of the wedge creates a weak expansion wave propagating out into the flow, too weak to be observable in the contour plots, that has the effect of pulling the triple point toward the wedge surface.

In the second stage of the simulation, shown in Figs. 10d–10f, the wedge is stopped and kept stationary at 16 deg while the flow converges to steady state. The plots are shown with respect to a characteristic time, in this case defined as the time ratio of the actual time to the time a wave traveling at the freestream sound speed travels the length of the wedge. A more detailed set of plots of the transition process are shown in Fig. 11. As the solution converges to the steady state, the triple point continues to approach the wall as the incident shock wave angle approaches the steady-state value. At $T = 0.5$, the incident shock wave angle is 33.47 deg, within measurement accuracy of the steady-state value. The Mach reflection terminates between $T = 0.5$ and 0.6. It is unknown whether the fact that the incident wave reaches steady state at approximately the same time as the termination of the Mach reflection has any significance and is worth further investigation. In this transition, the solution has to jump from state one on Fig. 9 to state two. The flow caters for this discontinuous jump by the initiation of a shock wave from the reflection point that propagates downstream, bending the reflected wave in the process. Note that this transitional shock wave must be traveling downstream. This is so that, relative to this shock wave, the fluid is flowing from right to left, from the low-pressure region to the high-pressure region.

In Figs. 11b and 11c, the remnants of the slipstream can be seen convecting downstream. If the Mach reflection had terminated without an inverse Mach reflection having developed, the slipstream would have reduced in size as the triple point approached the wall and would have vanished as the transition occurred. However, in this case, because the slipstream is directed away from the wall, it is left stranded when the Mach reflection terminates, and it washes downstream.

Conclusions

A study was performed of transition between regular and Mach reflection in time-dependent flows. The von Neumann and detachment criterion are well established as the theoretical limits for regular and Mach reflections in steady flows. In this study, the angle of the incident wave was varied continuously and the effect this had on the nature of transition was observed.

When the wedge was moved very slowly, essentially approximating a steady flow, transition in both cases occurred near the theoretical limits. The hysteresis phenomenon was successfully reproduced and potential issues that this could have in the simulation of steady flows were discussed.

As the rate of rotation was increased, transition from regular reflection was only observed after the detachment criterion had passed. It is likely that under these conditions the steady-state prediction of where detachment actually occurs becomes increasingly invalid as the rate of angle change increased.

Slowly decreasing the wedge angle resulted in a very slow decrease in the height of the Mach stem, such that the triple point had not yet reached the reflecting surface once the incident wave angle passed the von Neumann criterion. At this stage, the single Mach reflection becomes an inverse Mach reflection. This resulted in transition occurring away from the von Neumann criterion, which is the only point where a continuous transition is possible.

Whereas it is theoretically well established that transition has to be discontinuous away from the von Neumann criterion, this is not easily observed. It was possible to observe the effect of this transition in these simulations. In both cases, a shock wave was initiated at transition that traveled downstream from the reflection point.

For the study of transition with a changing incident wave angle, the most important development would be an analytical prediction of detachment in unsteady flows. In the absence of such a prediction, numerical solutions at high resolutions are essential to better predict when transition from regular reflection is actually occurring. A wider range of freestream Mach numbers should also be investigated.

References

- ¹Felthun, L., and Skews, B. W., "Transition Between Regular and Mach Reflections in Dynamic Compressible Flows," AIAA Paper 02-0549, Jan. 2002.
- ²Henderson, L. F., and Lozzi, A., "Experiments on Transition of Mach Reflection," *Journal of Fluid Mechanics*, Vol. 68, 1975, pp. 139–155.
- ³Hornung, H. G., Oertel, H., and Sandeman, R. J., "Transition to Mach Reflection of Shock Waves in Steady and Pseudosteady Flow with and Without Relaxation," *Journal of Fluid Mechanics*, Vol. 90, 1979, pp. 541–560.
- ⁴Chpoun, A., Passerel, D., Lengrand, J.-C., Li, H., Ben-Dor, G., "Mise en Evidence Experimentale et Numerique d'un Phenomene d'Hysteresis lors de la Transition Reflexion de Mach-Reflexion Reguliere," *Comptes Rendus de l'Académie des Sciences, Paris*, Vol. 319, 1994, pp. 1447–1453.
- ⁵Khotyanovsky, D. V., Kudryavtsev, A. N., and Ivanov, M. S., "Numerical Study of Transition Between Steady Regular and Mach Reflection Caused by Freestream Perturbations," *Proceedings of the 22nd International Symposium on Shock Waves*, Univ. of Southampton, Southampton, England, U.K., 1999, pp. 1261–1266.
- ⁶Ben-Dor, G., Ivanov, M., Vasilev, E. I., and Elperin, T., "Hysteresis Processes in the Regular Reflection \leftrightarrow Mach Reflection Transition in Steady Flows," *Progress in Aerospace Sciences*, Vol. 38, 2002, pp. 347–387.
- ⁷Luo, H., Baum, J. D., and Löhner, R., "An Improved Finite Volume Scheme for Compressible Flows on Unstructured Grids," AIAA Paper 95-0348, Jan. 1995.
- ⁸Barth, T. J., and Jespersen, D. C., "The Design and Application of Upwind Schemes on Unstructured Meshes," AIAA Paper 89-0366, Jan. 1989.
- ⁹Nkonga, B., and Guillard, H., "Godunov Type Method on Non-Structured Meshes for Three-Dimensional Moving Boundary Problems," *Computer Methods in Applied Mechanics and Engineering*, Vol. 113, 1994, pp. 183–204.
- ¹⁰Markelov, G. N., Pivkin, I. V., and Ivanov, M. S., "Impulsive Wedge Rotation Effects on the Transition from Regular to Mach Reflection," *Proceedings of the 22nd International Symposium on Shock Waves*, Univ. of Southampton, Southampton, England, U.K., 1999, pp. 1243–1248.

M. Sichel
Associate Editor